PSME model of parametric excitation of two-layer liquid in a tank

PSME Model of Parametric Excitation of Two-Layer Liquid in a Tank

Nima Vaziri[1,*], Ming-Jyh Chern[2,3], Alistair G. L. Borthwick[4]

[1] *Department of Physics, Islamic Azad University, Karaj Branch, Karaj, Iran*

[2] *Department of Mechanical Engineering, National Taiwan University of Science and Technology, 43 Sec. 4 Keelung Road, Taipei 10607, Taiwan*

[3] *Ecological Engineering Research Unit, National Taiwan University, No. 1 Sec. 4 Roosevelt Road, Taipei 10617, Taiwan*

[4] *Department of Civil and Environmental Engineering, University College Cork, Cork, Ireland*

[*] *E-mail: nima_vaziri@kiau.ac.ir; Tel: (98)-26-32554506; Fax: (886)-2-2737-6460*

Abstract

Internal waves driven by external excitation constitute important phenomena that are often encountered in environmental fluid mechanics. In this study, a pseudospectral σ-transformation model is used to simulate parametric excitation of stratified liquid in a two-layer rectangular tank. The σ-transformation maps the physical domain including the liquid free surface, the interface between the liquid layers, and the bed, onto a pair of fixed rectangular computational domains corresponding to the two layers. The governing equation and boundary conditions are discretised using Chebyshev collocation formulae. The numerical model is verified for two analytical sloshing problems: horizontal excitation of constant density liquid in a rectangular tank, and vertical excitation of

stratified liquid in a rectangular tank. A detailed analysis is provided of liquid motions in a shallow water tank due to excitations in the horizontal and the vertical directions. Results are presented from a parameter study on horizontal excitation of shallow liquid in a tank examining the influences of water depth, density difference, and pycnocline on the wave motions and patterns. It is found that wave elevations at the free surface and the internal density interface are relatively dependent on the water depth and the density difference. Also, the interface wave regime is changed at large values of density difference. Furthermore, wave regimes and patterns are considerably influenced by the pycnocline, especially when the excitation frequency is large. The present study demonstrates that a pseudospectral σ-transformation can accurately model non-linear sloshing waves in a two-layer rectangular tank.

Keywords: PSME method; Two-layer system; Parametric excitation, Stratification, Internal waves.

1. Introduction

When a partially-filled liquid container is subjected to external forcing, it can be susceptible to sloshing motion. The motion can become resonant as the tank excitation frequency approaches the natural frequency of the liquid within the tank. The case of surface waves, excited by either horizontal or vertical oscillations, has been the subject of many studies. Ibrahim (2005) provides a comprehensive review of the physics of free surface liquid sloshing. If such tanks are exposed to the environment, stratification may occur, and internal waves may develop.

The primary mechanisms for sloshing of internal waves are parametric excitation, resonance due to the bottom topology (see e.g. Ting 1992, McKee 1996, Alam & Mei 2007, and Alam *et al.* 2009) and resonance due to wave interactions (see e.g. Lewis *et al.* 1974, Hill & Foda 1996, and Jamali *et al.* 2003). Theoretical (e.g. Kravatsov & Sekerzh-Zenkovich 1996), experimental (e.g. Kalinichenko 1986, and Benielli & Sommeria 1998) and numerical (e.g. Valentine & Frandsen 2005) studies have been undertaken into parametric excitation of interfacial waves.

Spectral methods are highly accurate numerical techniques that are appropriate for solving certain problems in fluid mechanics (see e.g. the detailed reviews by Hussaini & Zang 1987 and Zang *et al.* 2011). The present study describes a Chebyshev pseudospectral matrix-element (PSME) model (following Ku & Hatziavramidis 1985, Chern *et al*. 1999 and Chern *et al*. 2012) of a two-layer density-stratified liquid in a rectangular tank. The model has been developed with the longer-term view of being able to simulate internal waves in an ocean or a lake caused by a large-scale external excitation such as an earthquake, submarine volcano, or underwater landslide. This work is motivated by the need for a better understanding of the parametric external excitation necessary for generation of internal waves using a fully non-linear model. The problem is an extension of the case of the motions of homogeneous liquid in a tank (Chern *et al*. 1999). Unlike the case of a non-stratified liquid, in a two-layer system there are two wave solutions [Nima, could you reword this more clearly??] at any arbitrary excitation frequency, relating to the free surface and interfacial motions. Herein, the physical domain is divided into two computational domains. A σ-transformation method maps

each domain onto a rectangle and therefore overcomes the problems of specifying the free surface and the interface explicitly. A consequence of the mapping is that the free surface and the interface cannot be overturning or breaking. The two liquid layers are assumed immiscible and the tank bed is flat.

The paper is structured as follows. Section 2 describes the mathematical model and its numerical solution using PSME. Section 3 outlines the verification of the model for two standard benchmark tests involving horizontal and vertical excitation of liquid in a tank. Section 4 presents numerical results for horizontal and vertical excitations of stratified shallow water in a tank. Section 5 covers a parameter study on surge excitation of stratified liquid in a tank, examining the influence of water depth, density difference, and the presence or absence of a pycnocline. Section 6 details the main conclusions.

2. Mathematical Model of Two-layer system in the Cartesian Domain

Figure 1 shows an illustration of the model tank of length a. The depths of the upper and the lower layers are d_1 and d_2, respectively. The densities of the layers are denoted ρ_1 and ρ_2. The interface is the pycnocline that separates the upper and the lower layers. At the interface, the liquid density changes abruptly from the upper layer (ρ_1) to the lower layer (ρ_2). In all cases (except Section 7) the depth of the pycnocline is less than 5 percent of the total tank depth and remains constant [does this mean that no waves are created in these cases???]. The characteristic depths of layers are measured from the centre of the pycnocline. For an incompressible, inviscid, and irrotational fluid, the velocity potential φ satisfies Laplace's equation,

$$\frac{\partial^2 \varphi_i}{\partial x^2} + \frac{\partial^2 \varphi_i}{\partial y^2} = 0, \tag{1}$$

where i is [1, 2] and refers to the layer number. At the solid lateral wall and bed boundaries, the velocity components are set to zero, such that

$$\frac{\partial \varphi_i}{\partial x} = 0 \text{ at } x = 0 \text{ and } x = a, \tag{2}$$

and

$$\frac{\partial \varphi_2}{\partial z} = 0 \text{ at } z = -d_2. \tag{3}$$

This means that the flow can slip along but cannot penetrate the wall. Consider a tank undergoing forced periodic motion defined by

$$X_{\text{tank}} = A_x \sin(\Omega_x t),$$

$$Z_{\text{tank}} = A_z \sin(\Omega_z t), \tag{4}$$

where A is the excitation amplitude, Ω is the excitation frequency, and t is time. The X_{tank} and Z_{tank} excitations refer to surge and heave, respectively. By differentiating Equations (4) twice with respect to time, the tank acceleration components, $\frac{\mathrm{d}^2 X_{\text{tank}}}{\mathrm{d}t^2}$ and $\frac{\mathrm{d}^2 Z_{\text{tank}}}{\mathrm{d}t^2}$, are obtained. The natural frequency of the two-layer model without surface tension is given by Lamb (1945) as

$$\omega_n^2 = \frac{n\pi(\rho_2 - \rho_1) g \tanh(n\pi d / 2a)}{(\rho_2 + \rho_1) a} \quad (n = 1, 2, \ldots), \tag{5}$$

in which d is the total still water depth and g is the acceleration due to gravity. The non-linear dynamic and kinematic free surface boundary conditions are

$$\frac{\partial \varphi_1}{\partial t} = -g\eta_1 - \frac{1}{2}\left[\left(\frac{\partial \varphi_1}{\partial x}\right)^2 + \left(\frac{\partial \varphi_1}{\partial z}\right)^2\right] - x\frac{\mathrm{d}^2 X_{\text{tank}}}{\mathrm{d}t^2} - z\frac{\mathrm{d}^2 Z_{\text{tank}}}{\mathrm{d}t^2} \text{ at } z = d_1 + \eta_1, \tag{6}$$

and

$$\frac{\partial \eta_1}{\partial t} = \frac{\partial \varphi_1}{\partial z} - \frac{\partial \varphi_1}{\partial x}\frac{\partial \eta_1}{\partial x} \text{ at } z = d_1 + \eta_1, \tag{7}$$

where η_1 is the free surface elevation above the still water level. The normal stress of the fluid must be continuous across the interface (Drazin, 2002). For an inviscid fluid, this means that pressure must be continuous at the interface. Taking the unsteady Bernoulli equation along a streamline, we have

$$\begin{aligned}&\rho_1\frac{\partial \varphi_1}{\partial t} + \rho_1 g\eta_2 + \frac{\rho_1}{2}\left[\left(\frac{\partial \varphi_1}{\partial x}\right)^2 + \left(\frac{\partial \varphi_1}{\partial z}\right)^2\right] + x\frac{\mathrm{d}^2 X_{\text{tank}}}{\mathrm{d}t^2} + z\frac{\mathrm{d}^2 Z_{\text{tank}}}{\mathrm{d}t^2} = \\ &\rho_2\frac{\partial \varphi_2}{\partial t} + \rho_2 g\eta_2 + \frac{\rho_2}{2}\left[\left(\frac{\partial \varphi_2}{\partial x}\right)^2 + \left(\frac{\partial \varphi_2}{\partial z}\right)^2\right] + x\frac{\mathrm{d}^2 X_{\text{tank}}}{\mathrm{d}t^2} + z\frac{\mathrm{d}^2 Z_{\text{tank}}}{\mathrm{d}t^2} \text{ at } z = \eta_2,\end{aligned} \tag{8}$$

where η_2 is the interface elevation. This equation specifies the relationship between the spatial and temporal periodicity in the behavioural boundary conditions. The kinematic interface boundary condition is same as Equation (7). Initial conditions for the velocity potential and free surface elevation are given by

$$\varphi_i(x, z, 0) = -x\left.\frac{\mathrm{d}X_{\text{tank}}}{\mathrm{d}t}\right|_{t=0}, \tag{9}$$

and

$$\eta_i(x,0)=0. \tag{10}$$

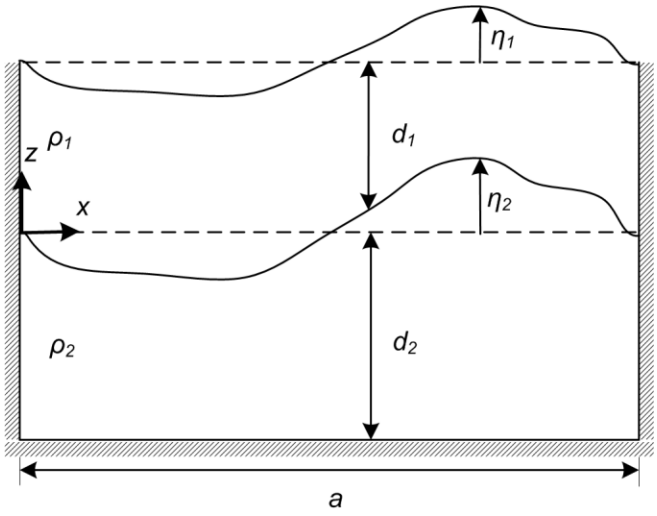

Figure 1 Schematic view of the tank.

2.1 σ- transformation

Following Philips (1957), the σ- transformation involves mapping the physical domain $x,z\in[0,a]\times[-d_i,\eta_i]$ onto a rectangular region $X,\sigma\in[-1,1]\times[-1,1]$ (Figure 2). The governing equation and its boundary conditions are altered accordingly to apply on the stretched grid system. The linear transformation is expressed as

$$\begin{aligned} X &= -1+\frac{2x}{a}, \\ \sigma &= -1+\frac{2(z+d_i)}{h_i}, \end{aligned} \tag{11}$$

where

$$h_i(x,t)=\eta_i(x,t)+d_i(x,t). \tag{12}$$

The σ- transformation for a two-dimensional model with an uneven bed (Vaziri *et al.*, 2011) is applied to both layers separately. The interface is the bed of the computational domain of the upper layer. Therefore, the topology of the bed of the upper layer is modified and must be updated at each time step. The σ- transform maps the velocity potential from $\varphi(x,z,t)$ in the physical domain onto $\Phi(X,\sigma,t)$ in the transformed domain. After applying the chain rule and rearranging, the transformed governing equation for each layer becomes

$$\left(\frac{2}{a}\right)^2\frac{\partial^2\Phi_i}{\partial X^2}+\left((2)\left(\frac{2}{a}\right)^2\left(\frac{2}{h_i}\right)\left(\frac{\partial d_i}{\partial X}\right)-(2)\left(\frac{2}{a}\right)^2\left(\frac{\sigma+1}{h_i}\right)\left(\frac{\partial \eta_i}{\partial X}+\frac{\partial d_i}{\partial X}\right)\right)\frac{\partial^2\Phi_i}{\partial\sigma\partial X}$$
$$+\left((-2)\left(\frac{2}{a}\right)^2\left(\frac{2}{h_i^2}\right)\left(\frac{\partial d}{\partial X}\right)\left(\frac{\partial \eta_i}{\partial X}+\frac{\partial d_i}{\partial X}\right)+\left(\frac{2}{a}\right)^2\left(\frac{2}{h_i}\right)\left(\frac{\partial^2 d_i}{\partial X^2}\right)+\left(\frac{2}{a}\right)^2\left(\frac{2(\sigma+1)}{h_i^2}\right)\left(\frac{\partial \eta_i}{\partial X}+\frac{\partial d_i}{\partial X}\right)^2\right.$$
$$-\left(\frac{2}{a}\right)^2\left(\frac{\sigma+1}{h_i}\right)\left(\frac{\partial^2\eta_i}{\partial X^2}+\frac{\partial^2 d_i}{\partial X^2}\right)-\left(\frac{2}{a}\right)^2\left(\frac{1}{h_i}\right)\left(\frac{2}{h_i}\right)\left(\frac{\partial d_i}{\partial X}\right)\left(\frac{\partial \eta_i}{\partial X}+\frac{\partial d_i}{\partial X}\right)+$$
$$\left.\left(\frac{2}{a}\right)^2\left(\frac{1}{h_i}\right)\left(\frac{\sigma+1}{h_i}\right)\left(\frac{\partial \eta_i}{\partial X}+\frac{\partial d_i}{\partial X}\right)^2\right)\frac{\partial\Phi_i}{\partial\sigma}+\left(\left(\frac{2}{a}\right)^2\left(\frac{2}{h_i}\right)^2\left(\frac{\partial d_i}{\partial X}\right)^2-\right.$$
$$\left.(2)\left(\frac{2}{a}\right)^2\left(\frac{2}{h_i}\right)\left(\frac{\partial d_i}{\partial X}\right)\left(\frac{\sigma+1}{h_i}\right)\left(\frac{\partial \eta_i}{\partial X}+\frac{\partial d_i}{\partial X}\right)+\left(\frac{2}{a}\right)^2\left(\frac{\sigma+1}{h_i}\right)^2\left(\frac{\partial \eta_i}{\partial X}+\frac{\partial d_i}{\partial X}\right)^2+\left(\frac{2}{h_i}\right)\right)\frac{\partial^2\Phi_i}{\partial\sigma^2}=0. \tag{13}$$

The boundary conditions, Equations (2), (3), (6), (7) and (8), are transformed in a similar fashion (see Vaziri *et al.*, 2011).

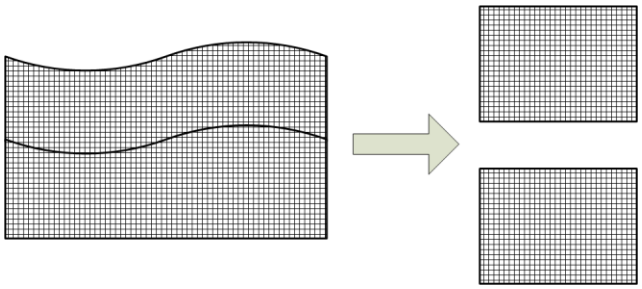

Figure 2 Transformation of the physical domain to the computational domain.

2.2 PSME modelling

The transformed governing equation and boundary conditions are discretised in the transformed domain using the Chebyshev collocation method where N and L are the total numbers of collocation points in the X, and σ directions. PSME discretisations are used to represent all spatial derivatives, such that $\frac{\partial \Phi}{\partial \sigma} = \sum_{m=0}^{L} \hat{\mathbf{G}}\boldsymbol{\sigma}_{km}^{(1)} \Phi_{ijm}$ and $\frac{\partial^2 \Phi}{\partial X^2} = \sum_{m=0}^{N} \hat{\mathbf{G}}\mathbf{X}_{im}^{(2)} \Phi_{mjk}$ wherein $\hat{\mathbf{G}}\boldsymbol{\sigma}_{km}^{(1)}$ and $\hat{\mathbf{G}}\mathbf{X}_{im}^{(2)}$ are Chebyshev matrix coefficients in the σ and X directions. A third-order Adam-Bashforth (AB3) scheme is used for time integration. Full details of the discretised equations are given by Chern *et al.* (2012).

Starting from a prescribed initial wave form, the solution procedure is as follows: (i) calculate free surface boundary values of Φ using Equation (6); (ii) calculate the interface values of Φ using Equation (8) for the upper layer; (iii) solve the discrete governing Equation (1) together with the wall boundary condition (2) for the upper layer by an iterative matrix solver; (iv) calculate the interface values of Φ using Equation (8) for the

bottom layer; (v) solve the discrete governing Equation (1) together with the wall and bed boundary conditions (2) and (3) for the bottom layer by an iterative matrix solver; (vi) update the surface and the interface elevations, η_i, using equation (7) and (vii) move forward one time step and return to (i). In this study, Successive Over-Relaxation (SOR) is used as the iterative matrix solver.

3. Model Verification Tests

The model is verified using two benchmark tests with analytical solutions: (i) the horizontal excitation of constant density liquid in a rectangular tank, and (ii) the vertical excitation of stratified water in a rectangular tank. It should be noted that in presenting the results, the non-dimensional time is defined as $t^* = \ldots$

3.1 Horizontal excitation of liquid of constant density in a rectangular tank

The first test concerns the motion of liquid of uniform density ($\rho_2/\rho_1 = 1.0$) in a tank subject to forced excitations that take place solely in the x-direction. The dimensions of the tank are such that the length to total still water depth ratio is $a/d = 2.0$. In the numerical model, each fluid layer has the same undisturbed depth, $d/2$. For homogeneous liquid in a 2D rectangular tank, the natural frequencies are (see e.g. Faltinsen 1978 and Wu *et al.* 1998)

$$\omega_n^2 = \frac{n\pi g \tanh(n\pi d/a)}{a} \quad (n = 1, 2, \ldots). \tag{14}$$

The verification test is carried out for non-dimensional forcing frequency $\Omega_x / \omega_1 = 0.999$ and non-dimensional amplitude $A_x / d = 0.001$. Figure 3 shows the agreement between the numerical prediction and the linear analytical solution (Faltinsen, 1978) of the free surface time history at the left hand tank wall. Very small amplitude oscillations can be seen developing at the layer interface, as the amplitude of free surface keeps increasing.

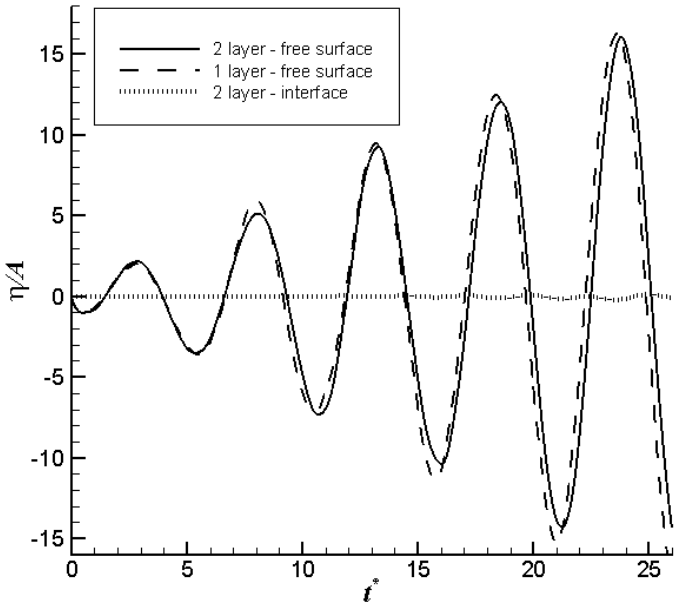

Figure 3 Liquid of uniform density undergoing vertical excitation: non-dimensional free surface and interface elevation time histories at the left hand tank wall for $\Omega_x / \omega_1 = 0.999$, $A_x / d = 0.001$, $a/d = 2.0$, $\rho_2/\rho_1 = 1.0$, $d_2/d_1 = 1.0$. Legend: — free surface, present model, – – free surface, analytical solution.

3.2 Vertical excitation of stratified liquid in a rectangular tank

The second test considers stratified shallow water in a tank, in which the density ratio is set to $\rho_2/\rho_1 = 1.03$, and the layer depth ratio $d_2/d_1 = 1$ [Nima, please check !!!]. The tank

length to overall still water depth ratio is a/d = 10. 0 and the non-dimensional amplitude is $A_z / d = 0.001$. The tank is excited vertically (heave excitation) with $\Omega_z / \omega_1 = 2.0$. Figure 4 shows the time history of the layer interface at the left hand tank wall. Resonance occurs at the interface, whose elevation increases exponentially after about t^* = 180. The maximum theoretical growth rate is given by $\exp(A_z\Omega^3 / 8g)$ (Benielli and Sommeria, 1998). Satisfactory agreement is obtained between the numerical and theoretical growth rates in Figure 4. Figure 5 depicts the periodic nature of the free surface waves with superimposed fluctuations that grow in amplitude with time, the growth phase becoming easily discernible after $t^* \sim 100$.

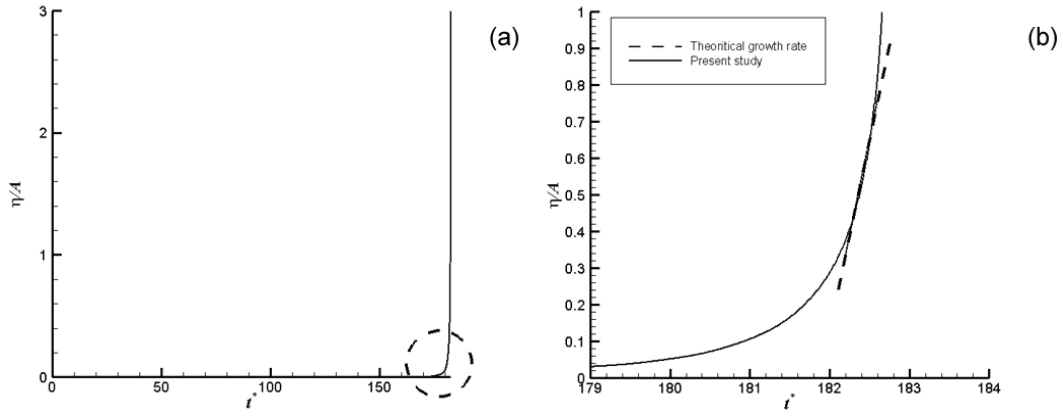

Figure 4 Stratified liquid undergoing vertical excitation, where $\Omega_z / \omega_1 = 2.0$, $A_z / d = 0.001$, a/d = 10.0, ρ_2/ρ_1 = 1.03, d_2/d_1 = 0.5: (a) non-dimensional layer interface elevation time history at the left hand tank wall; (b) enlarged section. Legend: — free surface, present model, – – free surface, analytical solution.

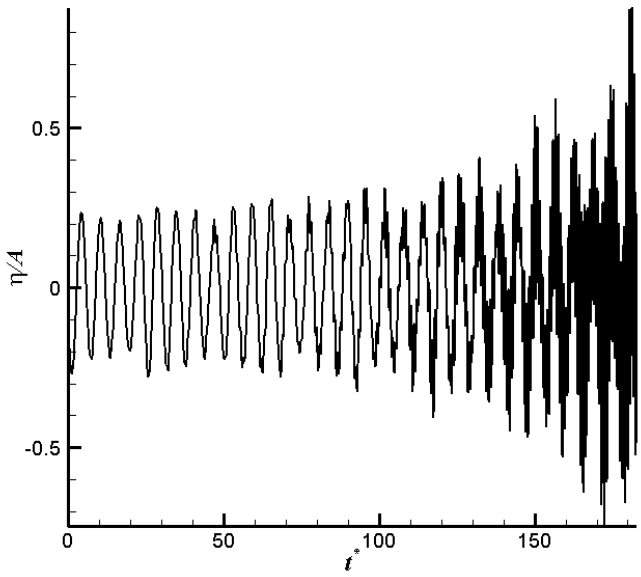

Figure 5 Stratified liquid undergoing vertical excitation, where $\Omega_z / \omega_1 = 2.0$, $A_z / d = 0.001$, $a/d = 10.0$, $\rho_2/\rho_1 = 1.03$, $d_2/d_1 = 0.5$: non-dimensional free surface elevation time history at the left hand tank wall.

4. Results

4.1 Horizontal Excitation of Stratified Shallow Water in a Tank

Consider the longitudinal (horizontal) excitation of water in a tank of dimensions $a/d =$ 10.0 undergoing forced sinusoidal displacements of non-dimensional amplitude $A_x/d =$ 0.001 at non-dimensional forcing frequency $\Omega_x / \omega_1 = 0.9999$. The density ratio, ρ_2/ρ_1, is set to 1.03 and the depth ratio, d_2/d_1, is 0.5 [Nima, is $d_1 = d_2$?; if so then ratio should be 1].

Previous studies have shown that the PSME method gives convergent and stable results over wide ranges of number of collocation points, and time step (see e.g. Chern *et al.*, 2012). Table 1 lists the parameters used to test for mesh convergence (number of

collocation points) and stability (time step). In all cases, the value of the relaxation factor is set to 1.3. Figure 6 presents time histories of the free surface (at the left hand tank wall) and the layer interface elevations (at the center of the tank) for all the mesh convergence test cases listed in Table 1. It can be seen that the spectral method gives convergent and stable results, except for Case c4. Based on these results, a collocated mesh of $40\times20\times10$ nodes and a non-dimensional time step, $\Delta t^* = \Delta t\sqrt{(g/d)}$, of 10^{-3} are selected for all the remaining cases. The simulations were performed on a workstation with four Intel Xeon 3.10 GHz CPUs and 8 GB RAM, and required less than 2 h CPU time to compute results up to a non-dimensional time of 50 for the selected case.

Table 1. Collocation point number and time step convergence test parameters.

Case	**N**	**L_1**	**L_2**	Δt^*
c1	20	10	5	0.001
c2	40	20	10	0.001
c3	60	30	15	0.001
c4	40	20	10	0.01
c5	40	20	10	0.0001

[Nima – please define N, L_1 and L_2 in Table 1]

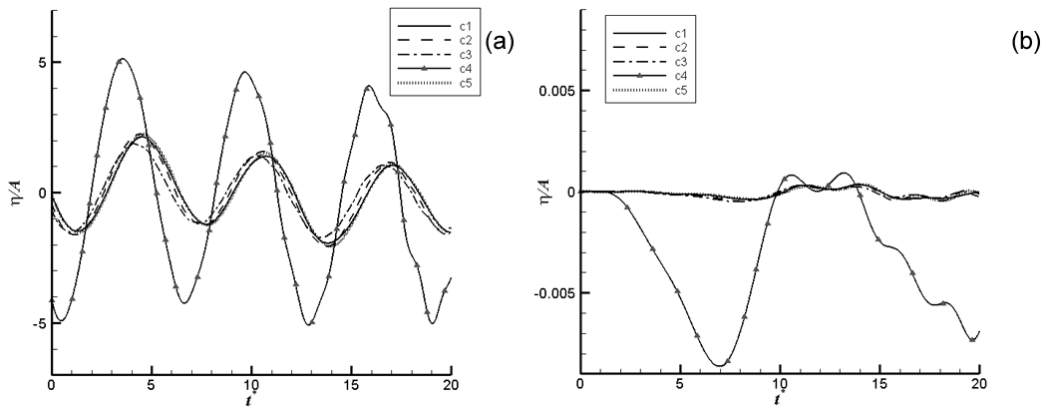

Figure 6 Convergence test results for horizontal excitation of stratified liquid in a rectangular tank: $\Omega_x / \omega_1 = 0.9999$, $A_x/d = 0.001$, $a/d = 10.0$, $\rho_2/\rho_1 = 1.03$, $d_2/d_1 = 1.0$. Time histories of (a) non-dimensional water free surface elevation (at the left hand tank wall) and (b) layer interface elevation (at the tank center), for varying N and Δt^*.

Figure 7 shows the almost periodic free surface elevation time histories obtained at the left hand wall and the center of the tank for an horizontal excitation frequency equal to $0.9999\omega_1$. Figure 8 displays the free surface wave profiles across the tank at different times at the beginning of the simulation ($t^* = 1, 2.5, 3.5, 4.5, 6$) and near the end of the simulation ($t^* = 80, 81, 82.5, 84$). The motions are almost planar. However, travelling waves are created at the two ends of the tank, and have amplitudes that increase gradually. Figure 9 shows the corresponding layer interface motions, where the travelling waves help induce very small amplitude (bursting) wave group motions of the layer interface at the center of the tank. Similar end wall travelling wave phenomena have previously been observed in heave excitation (see Benielli and Sommeria, 1998). The motion gradually evolves into almost standing waves at low values of A_x/d (Figure

10). After $t^* \sim 80$, the layer interface elevation abruptly increases at both ends of the tank, but the motion regime does not change thereafter until the end of the simulation at $t^* = 100$. This regime is almost that of seiche-related motions (Forel, 1895). Figure 11 depicts the velocity potential contours and the velocity vectors at $t^* = 25$. In the upper layer, because of the planar regime at the free surface, nearly symmetric patterns of contours and vectors are observed; but in the bottom layer, small amplitude standing waves occur at the layer interface driving almost chaotic motions in certain areas of the lower layer.

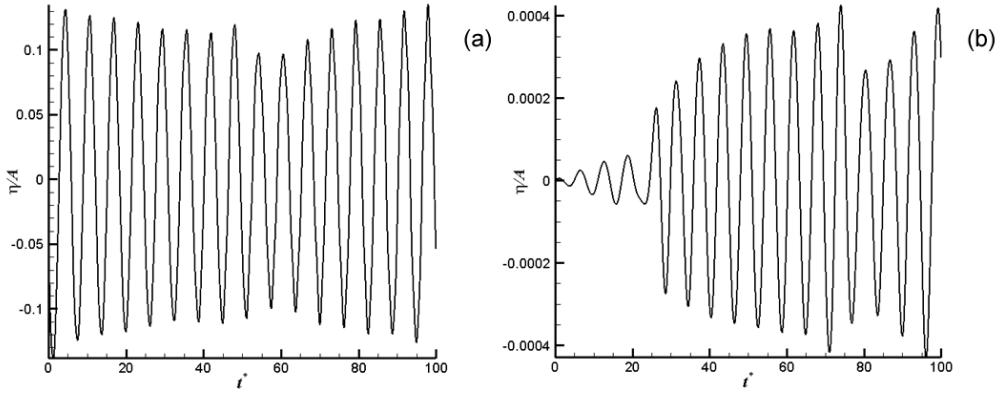

Figure 7 Horizontal excitation of stratified liquid in a rectangular tank: $\Omega_x / \omega_1 = 0.9999$, $A_x/d = 0.001$, $a/d = 10.0$, $\rho_2/\rho_1 = 1.03$, $d_2/d_1 = 1.0$. Non-dimensional free surface elevation time histories at (a) left hand tank wall, and (b) tank center.

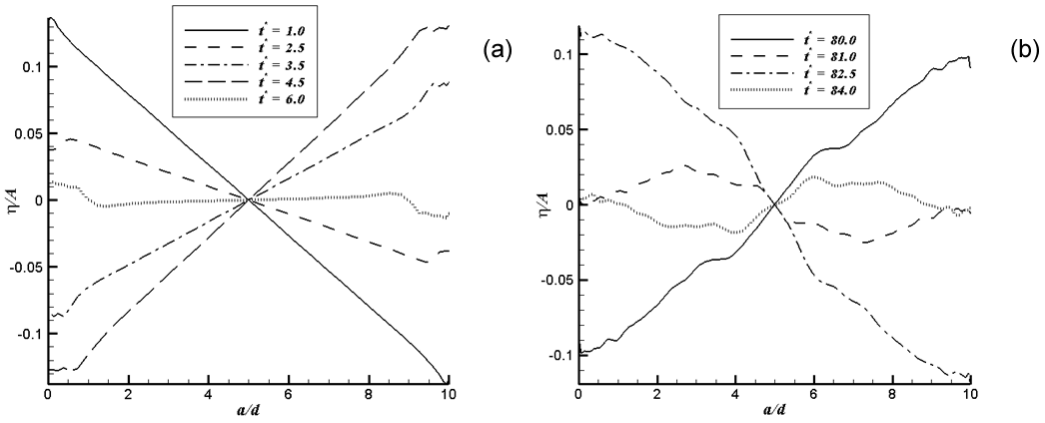

Figure 8 Horizontal excitation of stratified liquid in a rectangular tank: $\Omega_x / \omega_1 = 0.9999$, $A_x/d = 0.001$, $a/d = 10.0$, $\rho_2/\rho_1 = 1.03$, $d_2/d_1 = 1.0$. Non-dimensional free surface waves profiles at times (a) near the beginning of the simulation, and (b) near the end of the simulation.

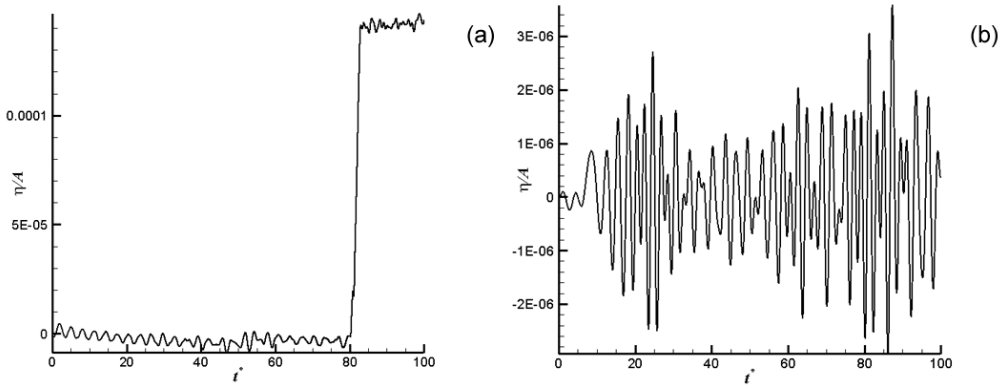

Figure 9 Horizontal excitation of stratified liquid in a rectangular tank: $\Omega_x / \omega_1 = 0.9999$, $A_x/d = 0.001$, $a/d = 10.0$, $\rho_2/\rho_1 = 1.03$, $d_2/d_1 = 1.0$. Non-dimensional layer interface elevation time histories at (a) left hand tank wall, and (b) tank center.

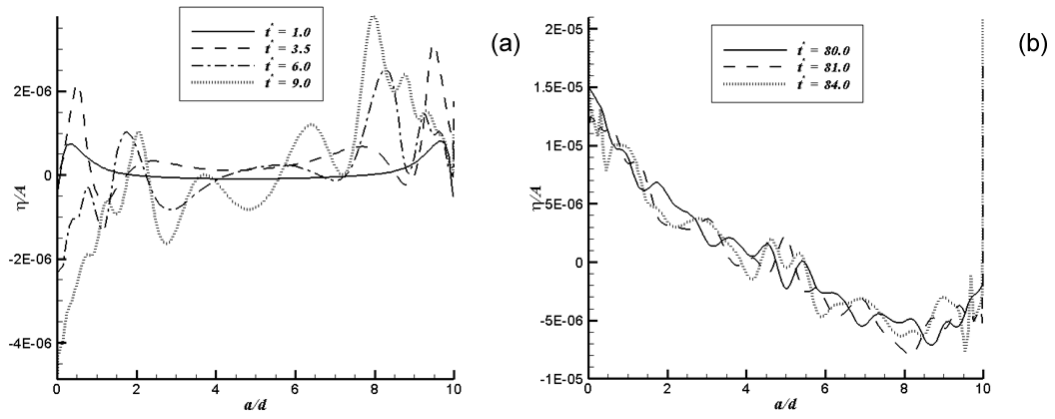

Figure 10 Horizontal excitation of stratified liquid in a rectangular tank: $\Omega_x / \omega_1 = 0.9999$, $A_x/d = 0.001$, $a/d = 10.0$, $\rho_2/\rho_1 = 1.03$, $d_2/d_1 = 1.0$. Non-dimensional layer interface waves profiles at times (a) near the beginning of the simulation, and (b) near the end of the simulation.

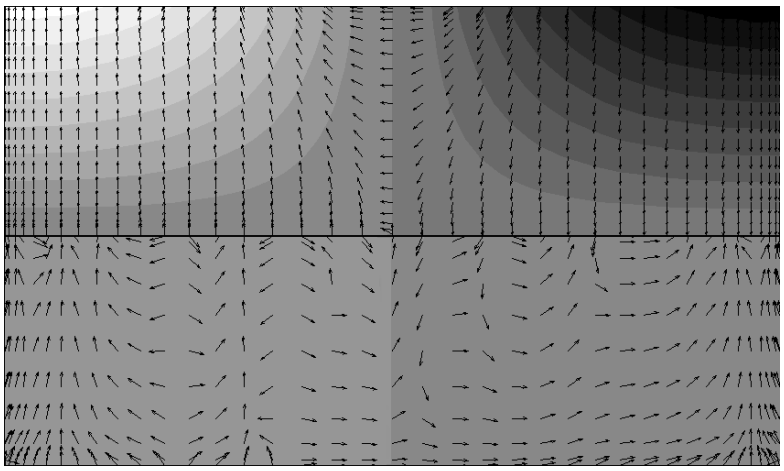

Figure 11 Horizontal excitation of stratified liquid in a rectangular tank: $\Omega_x / \omega_1 = 0.9999$, $A_x/d = 0.001$, $a/d = 10.0$, $\rho_2/\rho_1 = 1.03$, $d_2/d_1 = 1.0$. Velocity potential contours and velocity vectors at $t^* = 25$.

4.2 Vertical (Heave) Excitation of Stratified Shallow Water in a Tank

The tank is now excited solely in the vertical direction (heave) at a non-dimensional excitation frequency $\Omega_z / \omega_1 = 2.0$. Again, a/d = 10.0, ρ_2/ρ_1 = 1.03, d_2/d_1 = 1.0. The resulting free surface elevation and interface layer elevation time histories are depicted in Figure 12 – both the free surface and layer interface motions exhibit similar behaviour as to those obtained for the corresponding case of longitudinal excitation but with larger amplitude as would be expected due to the increased value of non-dimensional excitation frequency.

4.3 Simultaneous Horizontal and Vertical Excitation of Stratified Shallow Water in a Tank

Finally, the tank is excited in both directions simultaneously. The non-dimensional excitation frequencies in surge and heave are $\Omega_x / \omega_1 = 0.9999$ and $\Omega_z / \omega_1 = 2.0$. The corresponding non-dimensional excitation amplitudes are A_x/d = 0.001 and A_z/d = ???, Figure 13 depicts the free surface and the interface elevation time histories obtained at the left hand tank wall. The free surface motions form a standing wave pattern, with a much longer wave length than obtained in the previous cases. After $t^* \sim 40$, both the free surface elevation and layer interface elevation increase rapidly and the model is unable to simulate beyond $t^* = 41.2$. Similar phenomena in homogeneous flow have previously been observed under particular heave conditions and also for simultaneous excitation in vertical and horizontal directions (see e.g. Frandsen, 2004). Before a chaotic situation arises, the wave regimes at the free surface and the interface are planar and almost standing, respectively (see Figure 14). Later, high amplitude periodic waves develop at the free surface and the layer interface.

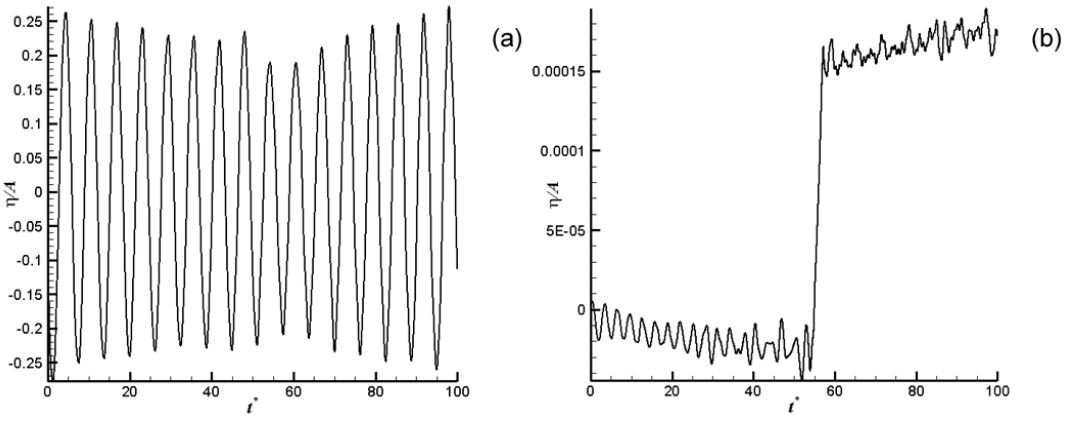

Figure 12 Vertical excitation of stratified liquid in a rectangular tank: $\Omega_z / \omega_1 = 2.0$, A_x/d = 0.001, a/d = 10.0, ρ_2/ρ_1 = 1.03, d_2/d_1 = 1.0. Non-dimensional elevation time histories at left hand tank wall: at (a) free surface, and (b) layer interface.

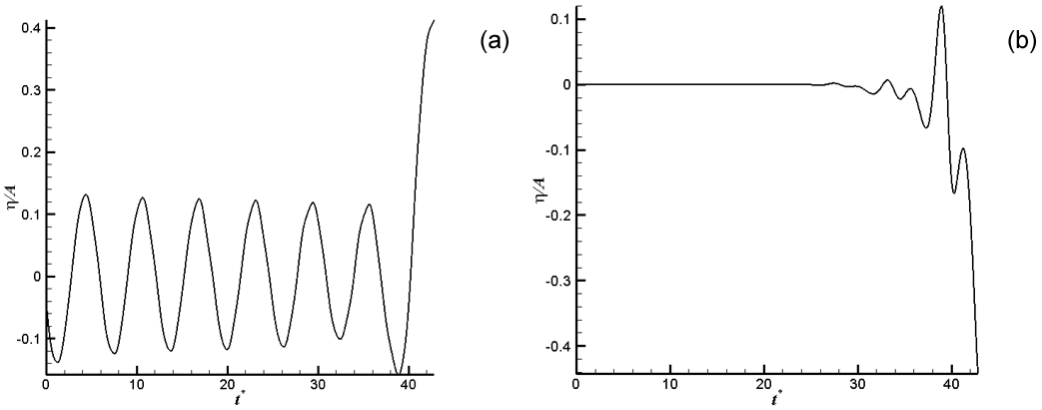

Figure 13 Simultaneous horizontal and vertical excitation of stratified liquid in a rectangular tank: $\Omega_x / \omega_1 = 0.9999$, $\Omega_z / \omega_1 = 2.0$, A_x/d = 0.001, A_z/d = ???, a/d = 10.0, ρ_2/ρ_1 = 1.03, d_2/d_1 = 1.0. Non-dimensional elevation time histories at left hand tank wall: at (a) free surface, and (b) layer interface.

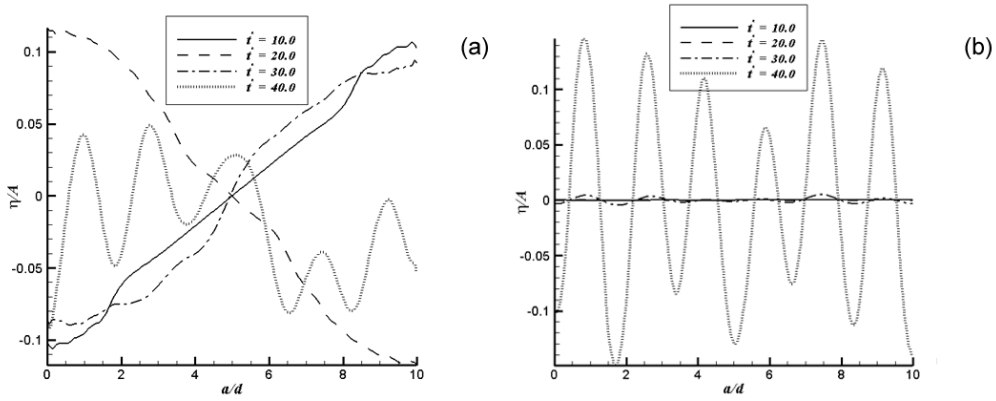

Figure 14 Simultaneous horizontal and vertical excitation of stratified liquid in a rectangular tank: $\Omega_x / \omega_1 = 0.9999$, $\Omega_z / \omega_1 = 2.0$, $A_x/d = 0.001$, A_z/d =???, $a/d = 10.0$, $\rho_2/\rho_1 = 1.03$, $d_2/d_1 = 1.0$. Non-dimensional (a) free surface and (b) interface wave profiles.

5. Parameter Study on Horizontal Excitation of Stratified Liquid in a Tank

5.1 Influence of water depth

It is well established that sloshing of homogeneous liquid in a tank is dependent on the ratio of still water depth to length of tank (e.g. see Faltinsen *et al.*, 2005). Here, we consider sloshing in a two-layer tank for four different ratios of depth to length ratio: d/a = 1/2 (deep water), 1/3 (finite depth), 1/5 (intermediate depth), and 1/10 (shallow water). The non-dimensional surge excitation amplitude is $A_x/d = 0.001$ and the excitation frequency is $\Omega_x = 0.9999\omega_1$. The density ratio is 1.03, and the depth ratio is 0.5 [Nima – please check this]. Figures 15 and 16 show the free surface and the layer interface elevation time histories at the center for all the depth ratios considered. The behavior of the free surface and layer interface motions of the stratified liquid is qualitatively similar to that obtained for homogeneous liquid in a tank subject to horizontal excitation in that the elevation amplitude increases monotonically as the depth to length ratio decreases.

The wave motion regimes are invariably planar at the free surface and almost standing waves at the later interface.

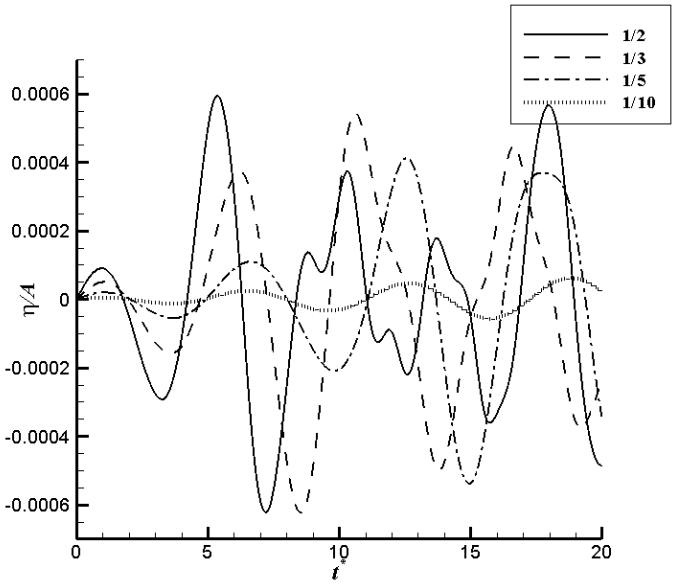

Figure 15 Parameter study on horizontal excitation of stratified liquid in a tank: $\Omega_x / \omega_1 = 0.9999$, $A_x/d = 0.001$, $\rho_2/\rho_1 = 1.03$, $d_2/d_1 = 1.0$. Non-dimensional free surface elevation time histories at the center of the tank for different depth/length ratios, d/a = 1/2, 1/3, 1/5 and 1/10.

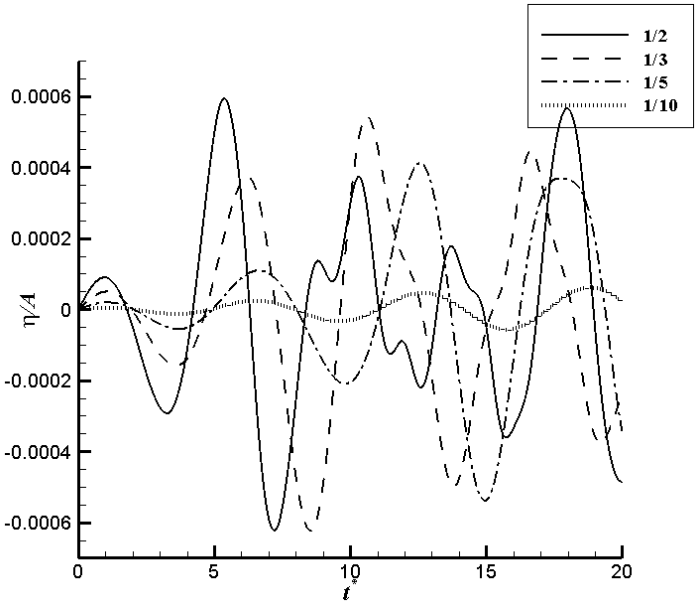

Figure 16 Parameter study on horizontal excitation of stratified liquid in a tank: $\Omega_x / \omega_1 = 0.9999$, $A_x/d = 0.001$, $\rho_2/\rho_1 = 1.03$, $d_2/d_1 = 1.0$. Non-dimensional layer interface elevation time histories at the center of the tank for different depth/length ratios, d/a = 1/2, 1/3, 1/5 and 1/10.

5.2 Influence of density

Next, we consider the effect of the density difference on the two-layer system sloshing in a tank of dimensions $a/d = 10.0$. Five different density ratios are selected: $\rho_2/\rho_1 = 1.01$, 1.03, 1.05, 1.10 and 1.50. The longitudinal excitation frequency is $\Omega_x = 0.9999\omega_1$ and the surge excitation amplitude is $A_x/d = 0.001$. The two layers have the same thickness equal to $d/2$, such that $d_2/d_1 = 1.0$ in all cases. Figures 17 and 18 present the time histories of free surface and layer interface elevations at the tank center for all density ratios considered.

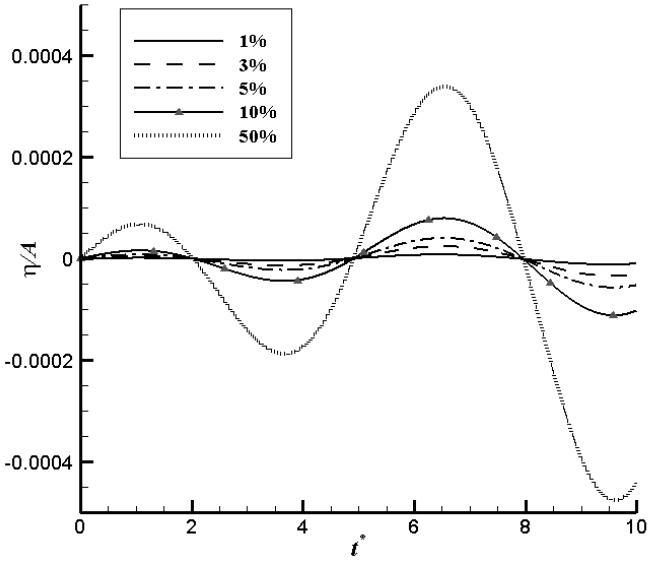

Figure 17 Parameter study on horizontal excitation of stratified liquid in a tank: a/d = 10.0, $\Omega_x / \omega_1 = 0.9999$, $A_x/d = 0.001$, $d_2/d_1 = 1.0$. Non-dimensional free surface elevation time histories at the center of the tank for different density differences ρ_2/ρ_1 = 1.01, 1.03, 1.05, 1.10 and 1.50.

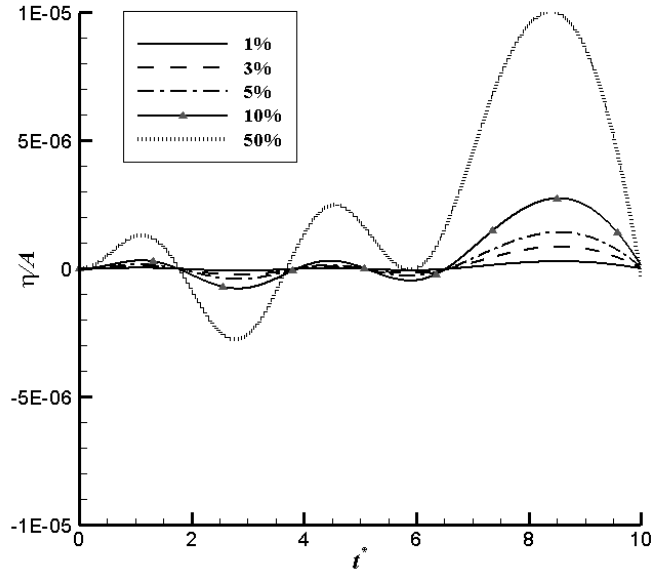

Figure 18 Parameter study on horizontal excitation of stratified liquid in a tank: a/d = 10.0, $\Omega_x / \omega_1 = 0.9999$, A_x/d = 0.001, d_2/d_1 = 1.0. Non-dimensional layer interface elevation time histories at the center of the tank for different density differences ρ_2/ρ_1 = 1.01, 1.03, 1.05, 1.10 and 1.50.

In all cases, the free surface motions are self-similar, except that the amplitude becomes amplified as the density difference increases. As would be expected, the amplitude of layer interface motions increases with density ratio. Furthermore, the wave motion pattern changes, as illustrated by Figure 19. Seiche-related behaviour is observed, leading finally to almost periodic waves when the density ratio $\rho_2/\rho_1 < 1.1$ (see previous discussion in Section 4). However, when $\rho_2/\rho_1 > 1.1$, the planar wave regime dominates with the layer interface motions qualitatively similar to the free surface motions, but with smaller frequency and amplitude.

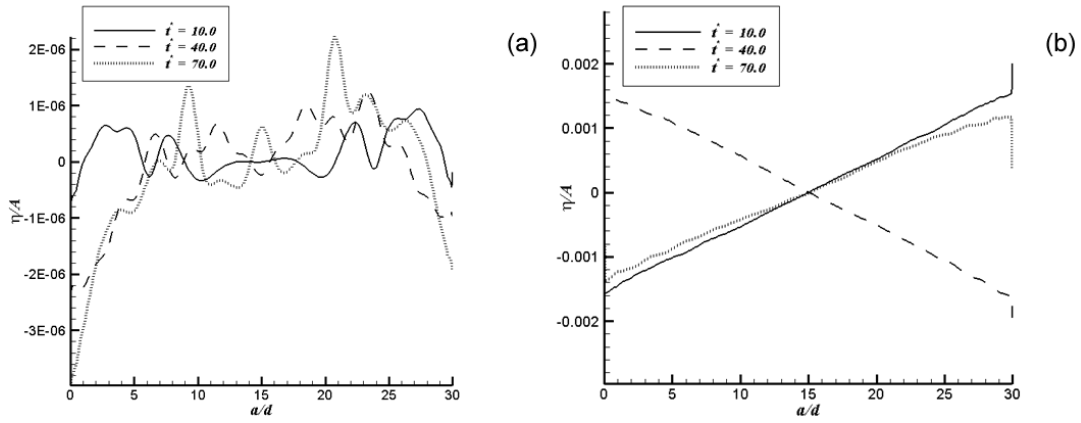

Figure 19 Parameter study on horizontal excitation of stratified liquid in a tank: a/d = 10.0, $\Omega_x / \omega_1 = 0.9999$, A_x/d = 0.001, d_2/d_1 = 1.0. Layer interface wave profiles at non-dimensional times t^* = 10, 40, and 70: (a) ρ_2/ρ_1 = 1.01, (b) ρ_2/ρ_1 = 1.50.

5.3 Effect of pycnocline

In all the above cases, the layer interface is the pycnocline that separates the upper and the lower layer and it is assumed that this layer is stable until the end of the simulation. The final part of the parameter study examines the influence of the pycnocline on the sloshing properties. First, two cases are considered: one where the pycnocline is present, the second where the pycnocline does not exist. The non-dimensional excitation frequency is $\Omega_x / \omega_1 = 0.9999$, non-dimensional excitation amplitude $A_x/d = 0.001$, tank length to still water depth ratio $a/d = 10.0$, and frequency ratio $\rho_2/\rho_1 = 1.03$. Section 4.1 has previously discussed results for the tank with the pycnocline present (see Figures 7 to 11). Figure 20 depicts the free surface and the interface elevation time histories at the center of the tank in the absence of a pycnocline. The wave behaviour is almost same with or without the pycnocline present, except that the free surface elevation amplitude decreases while the layer interface elevation increases when the pycnocline is not present.

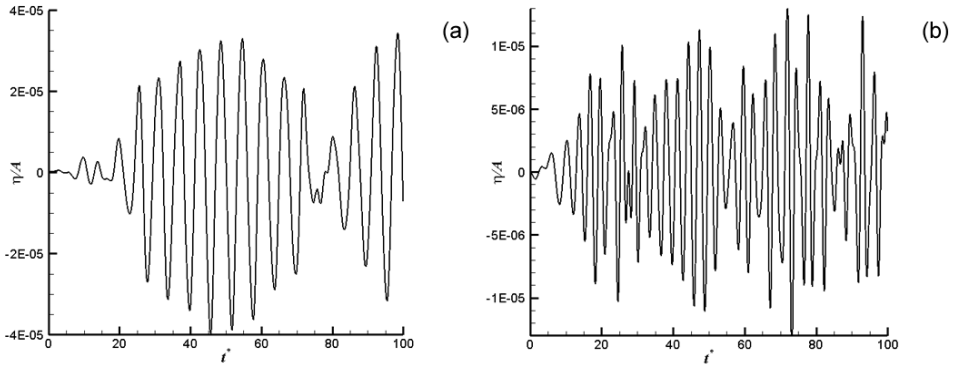

Figure 20 Parameter study on horizontal excitation of liquid in a tank: $a/d = 10.0$, $\Omega_x / \omega_1 = 0.9999$, $A_x/d = 0.001$, $\rho_2/\rho_1 = 1.03$, $d_2/d_1 = 1.0$. Non-dimensional (a) free

surface and (b) interface elevation time histories at the center of the tank without pycnocline.

Next, the tank is excited at a frequency of 0.6846 rad/s. This value is equal to the natural frequency of the tank containing liquid of uniform density, and is about 11 times larger than the natural frequency of the two-layer model tank. Figure 21 shows the free surface and the layer interface elevation time histories at the left hand side of the tank when the pycnocline is present. Large amplitude periodic waves are created at the free surface, which is to be expected because the excitation frequency in this case is much larger than the natural frequency of this tank. At the layer interface, the wave pattern is almost same as that at the free surface but with smaller amplitude and at lower frequency. The wave regimes at both the free surface and the layer interface are planar. Turning now to the case where the pycnocline is omitted, the free surface motions do not change but resonance occurs at the layer interface (Figure 22). These results indicate that resonance can be induced at the density layer interface when the pycnocline does not exist or disappears, provided the excitation force is sufficiently large.

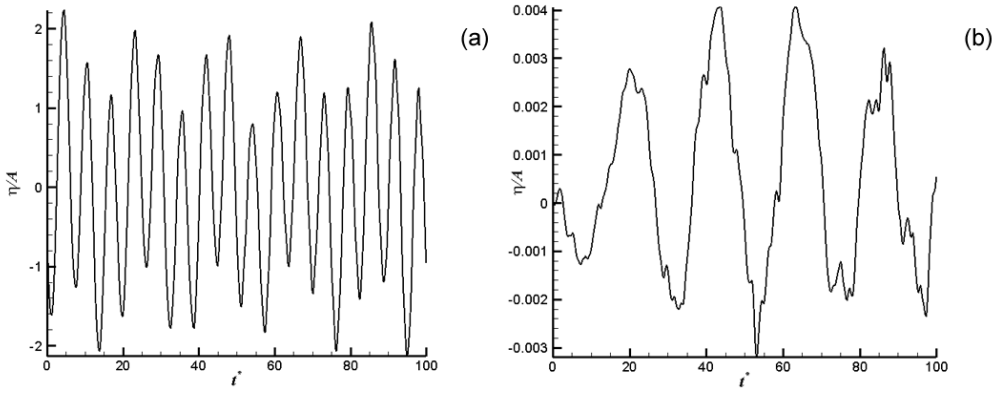

Figure 21 Parameter study on horizontal excitation of stratified liquid in a tank: a/d = 10.0, $\Omega_x = 0.6846\,\text{rad/s}$, A_x/d = ????, ρ_2/ρ_1 = 1.03, d_2/d_1 = 1.0. Non-dimensional (a) free surface and (b) interface elevation time histories at the left hand side of the tank, in which the pycnocline is present.

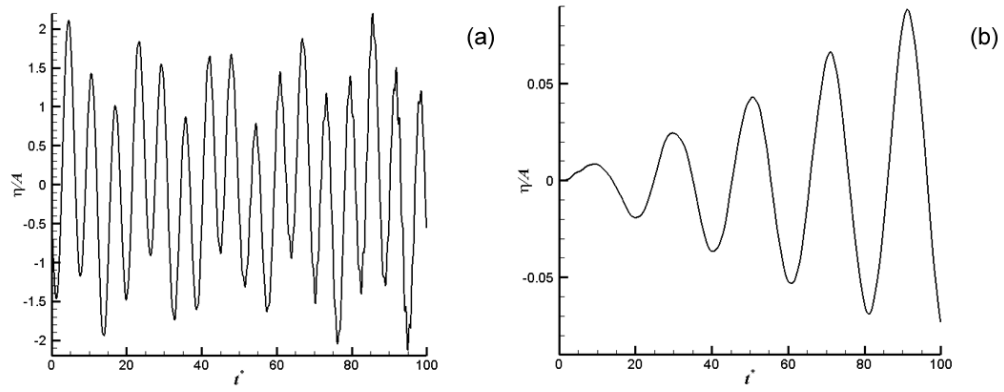

Figure 22 Parameter study on horizontal excitation of stratified liquid in a tank: a/d = 10.0, $\Omega_x = 0.6846\,\text{rad/s}$, A_x/d = ????, ρ_2/ρ_1 = 1.03, d_2/d_1 = 1.0. Non-dimensional (a) free surface and (b) interface elevation time histories at the left hand side of the tank, in which the pycnocline is absent.

6. Conclusions

A pseudospectral σ-transformation model has been used to simulate parametric excitation of stratified liquid in a 2D rectangular tank. The model was verified against analytical solutions for surge sloshing of homogeneous liquid in a rectangular tank and heave excitation of stratified liquid in a two-layer tank. Spectral grid convergence and numerical stability tests were carried out, and the results demonstrate that the model provides reasonably accurate predictions for a wide range of collocation points and time

steps. Simulations were the undertaken of solely horizontal and then solely vertical excitations of stratified liquid in a shallow water tank, where $a/d = 10.0$. In general, nearly standing waves were created at the free surface but the layer interface motions were seiche-like. When surge and heave excitations were simultaneously imposed, sloshing at the layer interface became significant. A parameter study investigated the effects of altering the water depth, the density ratio, and the pycnocline on the wave regime and the wave pattern of liquid in a rectangular tank. The results indicate that the amplitudes of free surface and the layer interface motions decrease as the ratio of depth to length increases; and the amplitudes of free surface and the layer interface motions increase as the density difference between the layers increases. Moreover, when the density ratio $\rho_2/\rho_1 > 1.1$, the wave regime at the layer interface alters to a planar mode. Turning to the effect of the pycnocline, the results demonstrate that resonance can be induced at the layer interface when the pycnocline does not exist, provided the excitation frequency is sufficiently large.

In short, the present study has demonstrated the capability of the PSME method to simulate the behaviour of stratified liquid undergoing parametric forced excitation in a two-layer rectangular tank. The results show that liquid motions in shallow containers strongly depend on the pycnocline at large values of excitation frequency.

Acknowledgments – This study was supported by Islamic Azad University – Karaj Branch research project titled "PSME modelling of a 3D tank with uneven bed".

References

Alam M. R., Liu Y., Yue D. K. P., 2009. Bragg resonance of waves in a two-layer fluid propagating over bottom ripples. Part I I. Numerical simulation. J. Fluid Mech. 624, 225-253.

Alam M. R., Mei C. C., 2007. Attenuation of long interfacial waves over a randomly rough seabed. J. Fluid Mech. 587, 73-96.

Benielli D., Sommeria J., 1998. Excitation and breaking of internal gravity waves by parametric instability. J. Fluid Mech. 374, 117-144.

Chern M. J., Borthwick A. G. L., Eatock Taylor R., 1999. A pseudospectral σ-transformation model of 2D nonlinear waves. Journal of Fluids and Structures 13, 607–630.

Chern M. J., Vaziri N., Syamsuri S., Borthwick A. G. L., 2012. Pseudospectral solution for three-dimensional non-linear sloshing in shallow water rectangular tank, J. Fluid. Struct. (In press).

Drazin P. G., 2002. Introduction to hydrodynamic stability. Cambridge University Press, Cambridge, England.

Faltinsen O. M., 1978. A numerical non-linear method of sloshing in tanks with two-dimensional flow. Journal of Ship Research 22(3), 193–202.

Faltinsen O. M., Rognebakke O. F., Timokha A. N., 2005. Classification of three-dimensional non-linear sloshing in a square-base tank with finite depth. Journal of Fluids and Structures 20(1), 81–103.

Forel F. A., 1895. Le Léman: Monographie Limnologique. Rouge, Lausanne.

Frandsen J. B., 2004. Sloshing motions in excited tanks. Journal of Computational Physics 196(1), 53-87.

Hill D. F., Foda M. A., 1996. Subharmonic resonance of short internal standing waves by progressive surface waves. J. Fluid Mech. 321, 217-233.

Hussaini M. Y., Zang T. A., 1987. Spectral methods in fluid dynamics. Annual Review of Fluid Mechanics 19, 339–367.

Ibrahim R. A., 2005. Liquid sloshing dynamics: theory and applications, Cambridge University Press, Cambridge.

Jamali M., Lawrence G. A., Seymour B., 2003. A note on the resonant interaction between a surface wave and two interfacial waves. J. Fluid Mech. 491, 19-25.

Kalinichenko, Y. A., 1986. Laboratory investigation of parametric instability in a two-layer fluid. Izv. Acad. Sci. USSR Atmos. Ocean. Phys. 22, 155-158.

Kravtsov A. V., Sekerzhi-Zenkovich S. Y., 1996. Parametric excitation of the oscillations of a viscous continuously stratified fluid in a closed vessel, J. Appl. Math. Mech. 60(3), 449-454.

Ku H. C., Hatziavramidis D., 1985. Solutions of the 2-dimensional Navier-Stokes equations by Chebyshev expansion methods. Computers & Fluids 13(1), 99–113.

Lamb, H. 1932 Hydrodynamics. 6th Ed., Dover, New York.

Lewis J. E., Lake B. M., Ko D. R. S., 1974. On the interaction of internal waves and surface gravity waves. J. Fluid Mech. 63(4), 773-800.

McKee W. D., 1996. Bragg resonances in two-layer fluid. J. Austral. Math. Soc. Sec. B 37(3), 334-345.

Philips N. A., 1957. A coordinate system having some special advantages for numerical forecasting, J. Appl. Meteorol. 14, 184–185.

Ting F. C. K., 1992. On forced internal waves in a rectangular trench. J. Fluid Mech. 255, 255-283.

Valentine D. T., Frandsen J. B., 2005. Nonlinear free-surface and internal-viscous sloshing. J. offshore Mech. Arct. Eng. 127, 141149.

Vaziri, N., Chern, M. J. and Borthwick, A. G. L., 2011. Pseudospectral σ-transformation model of solitary waves in a tank with uneven bed. Computers and Fluids, 49(1), 197-202.

Wu G. X., Ma Q. W., Eatock Taylor R., 1998. Numerical simulation of sloshing waves in a 3D tank based on a finite element method. Applied Ocean Research 20(6), 337–355.

Zhang, W., Xi, G., Zhang, C. and Huang, Z., 2011. A high-accuracy temporal–spatial pseudospectral method for time-periodic unsteady fluid flow and heat transfer problems. International Journal of Computational Fluid Dynamics, 25(4): 191-206.